Radiation Measurements 45 (2010) 78–82

Contents lists available at ScienceDirect

Radiation Measurements

journal homepage: www.elsevier.com/locate/radmeas

Characterization of a fiberoptic radiotherapy dosimetry probe based on Mg_2SiO_4:Tb

P. Molina [a,b], M. Prokic [c], J. Marcazzó [a,b], M. Santiago [a,b,*]

[a] Instituto de Física Arroyo Seco-UNICEN, Pinto 399, 7000 Tandil, Argentina
[b] Consejo Nacional de Investigaciones Científicas y Técnicas (CONICET), Argentina
[c] Institute of Nuclear Sciences, Vinca, P.O. Box 522, 11000 Belgrade, Serbia

ARTICLE INFO

Article history:
Received 16 June 2009
Received in revised form
17 November 2009
Accepted 25 November 2009

Keywords:
Radioluminescence
Magnesium orthosilicate
Dosimetry

ABSTRACT

In this work the feasibility of using Mg_2SiO_4:Tb as a fiberoptic radioluminescent (RL) dosimetry probe for real-time dosimetry has been investigated for the first time. In particular, the stability of the RL signal after repeated use, the spectrum of the RL emission and the dose-rate response curve of a Mg_2SiO_4:Tb-based fiberoptic probe have been determined. The probe has been also used to obtain a percentage dose depth curve in a water phantom and its performance has been compared to that of a standard ion chamber. Besides, its absolute RL yield has been compared to that of an RL probe based on the commercial Al_2O_3:C phosphor.

1. Introduction

The increasingly sophisticated techniques employed today in radiotherapy claim for the development of dosimetry systems suitable for in-vivo, real-time dose assessment (Beddar, 2007). The recently established fiberoptic dosimetry (FOD) method offers the potential to fulfill these requirements. This technique is based on the use of an efficient scintillating material, which is placed at the point of interest either inside or close to the patient. During irradiation, part of the energy absorbed by the scintillator is re-emitted as light of characteristic wavelength. This effect is known as radioluminescence (RL). An optical fiber, to which the scintillator is coupled, transports the emitted light out of the irradiation room, where a suitable high-gain light detector collects the RL yield. Generally the intensity of the scintillation light is proportional to the dose rate, what makes the system suitable for dosimetry. Overall, the FOD technique shows interesting characteristics: a) the small size of the detector permits accurate dose measurements in regions of high dose gradients, b) the system does not rely on any external high-voltage bias, c) its rugged design makes it suitable for the routine tasks carried out by radiotherapy technicians, d) since the reading is obtained during irradiation, the FOD technique allows for in-vivo and real-time dosimetry (Justus et al., 2004).

Many materials have been investigated as possible FOD dosimeters: Cu^{1+}-doped quartz (Justus et al., 2004), plastic scintillators (Archambault et al., 2006), scintillating fibers (Frelin et al., 2006), Ce^{3+}-doped SiO_2 optical fibers (Mones et al., 2006), Tb^{3+}-doped fluorides (Marcazzó et al., 2007), carbon-doped Al_2O_3 (Aznar et al., 2005; Damkjær et al., 2008; Marckmann et al., 2006), etc. Among them Al_2O_3:C has undoubtedly become the most investigated one and many reports show that it is a promising material for in-vivo, real-time dosimetry. However, some dependence of its response as function of the accumulated dose requires corrections through an algorithm to obtain precise dose-rate assessment (Damkjær et al., 2008). Different commercially available thermoluminescent dosimeters, namely, TLD-100, TLD-200, BeO, etc., have been also investigated. However, their RL yield is too poor to be suitable for RL dosimetry (Erfurt and Krbetschek, 2002; Marcazzó et al., 2007).

The main drawback of the FOD technique has to do with the spurious luminescence arriving at the light detector, which adds to the RL from the scintillator. This light, which is known as stem effect, has two contributions. The first one is the intrinsic luminescence generated in the optical fiber by the ionizing radiation and the second one is the Cherenkov emission. The latter is usually the most relevant component of the stem effect and becomes more important in the blue region of the spectrum, since the intensity of the Cherenkov emission is proportional to the inverse of the third power of the wavelength (De Boer et al., 1993). Since the stem effect depends on the length and relative position of the portion of irradiated fiber with respect to the therapy beam, it is not univocally

* Corresponding author. Instituto de Física Arroyo Seco-UNICEN, Pinto 399, 7000 Tandil, Argentina. Tel.: +54 2293 439660; fax: +54 2293 439669.
E-mail address: msantiag@exa.unicen.edu.ar (M. Santiago).

1350-4487/$ – see front matter © 2009 Elsevier Ltd. All rights reserved.
doi:10.1016/j.radmeas.2009.11.040

related to the dose rate at the sensitive end of the FOD probe. For this reason its contribution must be removed in order to obtain a measurement, which can be reliably linked to the dose rate.

Several methods have been put forward in order to get rid of the stem effect. The simplest method consists in using a second optical fiber without any scintillator at its extreme, say, a dummy fiber, which is placed in the same position as the FOD probe. During irradiation the dummy fiber only collects the spurious light and its signal is subtracted from that of the FOD probe in order to obtain the actual RL emission of the scintillator. Although very effective and robust, this method increases the final size of the probe, which precludes its use in those cases where high dose gradients are expected. Another removing method consists in simply filtering the light arriving at the light detector by means of optical filters, which cut off the spectral components of the stem effect. For this technique to be useful, the characteristic emission of the scintillator should be situated at longer wavelengths than the stem effect. A third technique for removing the stem effect, known as gated filtering, is only valid when the FOD probe is used for dosimetry in a linear accelerator (LINAC). LINACs emit radiation as a train of pulses, the dose rate being determined by the pulse frequency. Since the spurious luminescence is a short-lived effect, it is only important during the LINAC pulses. The gated filtering method consists in measuring the RL only during the time intervals between the radiation pulses. This technique has been successfully employed, for instance, to remove the stem effect in FOD probes in LINACs (Clift et al., 2002; Justus et al., 2004; Andersen et al., 2006; Damkjær et al., 2008).

Since the seventies Mg_2SiO_4:Tb has been well known for its high efficiency as thermoluminescent (TL) dosimeter (Bhasin et al., 1976). Recently, an optimal preparation of this TL phosphor has been reported, which shows the highest TL efficiency for this compound (Prokic and Yukihara, 2008). The optically stimulated luminescence (OSL) of Mg_2SiO_4:Tb has been also investigated (Mittani et al., 2008). In particular, Mg_2SiO_4:Tb fulfills the preliminary requirements to be taken as a promissory OSL dosimeter. Other luminescence properties of Mg_2SiO_4:Tb, which could be of interest in dosimetry, such as its radioluminescence (RL), have been never explored.

In this work the feasibility of using terbium-doped magnesium silicate (Mg_2SiO_4:Tb) as a FOD RL dosimeter has been investigated for the first time. In this context, a Mg_2SiO_4:Tb-based FOD probe has been fabricated and its response under ^{60}Co irradiation at a radiotherapy facility has been studied. In particular, its RL yield has been obtained and compared to that of a FOD probe based on commercial Al_2O_3:C crystals. Besides, the spectrum and stability of the RL emission have been determined. Finally, the FOD probe has been commissioned to obtain the PDD curve in a water phantom and the result has been compared to that obtained in identical conditions by means of a standard ionizing chamber.

2. Materials and methods

The terbium-doped silicate samples used in this work were developed by M. Prokic at the Institute of Nuclear Science, Vinca, Belgrade (Mittani et al., 2008). They were sintered for 1 h at 1660 °C in air, under slow heating rate. The resulting phosphor then was crushed and sieved in grains sized between 75 and 200 microns. By cold pressing the resulting polycrystalline material was shaped into pellets 4 mm diameter and 0.80 or 0.40 mm thickness, which were sintered under the same conditions as during the preparation of the polycrystalline phosphor. The final sintered pellets are opaque and very hard.

In order to fabricate the FOD probes 1 mm^3 pieces were cut from a Mg_2SiO_4:Tb pellet and glued to one of the ends of a plastic core optical fiber (PMMA, 980 microns diameter core, and 2 mm diameter outer jacket). The scintillator was optically shielded with an opaque, water resistant coating in order to avoid external light. Identical FOD probes were fabricated by using commercial (Landauer Inc.) Al_2O_3:C rods (1 mm diameter, 2 mm length).

Irradiation of the RL probes was performed in-situ (radiotherapy facility) employing a Theratron 80 ^{60}Co source, which renders 0.35 Gy min^{-1} at 5 mm water depth (80 cm SSD, source to surface distance). The RL signal from the FOD probes was measured by means of a Hammamatsu H9319 photon counting photomultiplier tube (PMT) having sensitivity between 300 and 850 nm. In order to remove the spurious contribution due to the stem effect emission a second optical fiber probe having no scintillating sample at its end was used. This dummy probe was placed close to the FOD probe during the experiments and its signal was subtracted from the FOD probe signal in order to obtain the actual RL yield. In all cases, the signal of the dummy probe was found to be less than 10% the signal of the RL probes.

Unless specified otherwise all measurements were carried out in a water phantom (Civco MT-100) at room temperature under the following reference conditions, namely, 10×10 cm^2 field and 80 cm SSD (source to surface distance). In all cases the end of the FOD probe containing the scintillator (sensitive end) was placed at 5 mm water depth and the fiber was perpendicularly oriented with respect to the beam axis.

The percentage depth dose (PDD) curve was determined at different depths in the water phantom by means of a manual depth dose apparatus (0.1 mm resolution). PDD profiles were determined from surface down to 100 mm, under reference conditions. A PTW 30013 Farmer-type ionization chamber and a PTW UNIDOS E electrometer were used for reference dose-rate measurements.

The spectrum of the RL emission was measured by means of an Acton Research SP-2155 0.15 m monochromator with a resolution of 10 nm. The Hamamatsu H9319 photon counting placed at the exit slit was employed to detect the scattered light. The sample was placed at the entrance slit and irradiated by means of the ^{90}Sr source, which was situated 1 cm away from the sample.

3. Results and discussion

Before carrying out the experiments both the Mg_2SiO_4:Tb and Al_2O_3:C FOD probes were dosed (stabilized) up to 100 Gy at the ^{60}Co source. According to the literature at this dose level the traps involved in the TL of both materials reach saturation (Yukihara et al., 2003; Prokic and Yukihara, 2008). It is expected that after this pre-irradiation process possible transient behavior of the RL emission related to partial trap filling could be reduced.

In Fig. 1 the RL curves of the Mg_2SiO_4:Tb and Al_2O_3:C FOD probes measured under reference conditions are shown. As can be seen, the maximum RL intensity is of the same order for both probes. However, in the case of the Mg_2SiO_4:Tb probe the raising time, say, the time necessary for the RL signal to reach its maximum value, is appreciably shorter. In fact, while the raising time for the Mg_2SiO_4:Tb probe is of the order of 1 s, the corresponding value for the Al_2O_3:C probe is approximately 10 times longer. Although useful, this result provides only a rough comparison of the RL yield between both kinds of probes, by taking into account that the shape of the samples glued at the end of the optical fiber is slightly different in each case. Besides, the light collection efficiency is also possible different, since the commercial Al_2O_3:C rods are transparent, while the Mg_2SiO_4:Tb pellets are opaque.

In order to study the response stability after repeated use of the Mg_2SiO_4:Tb probe, its RL emission has been recorded during eight consecutive irradiation cycles. The exposure time was 60 s and the lapse between irradiations 120 s. Each time the RL intensity has

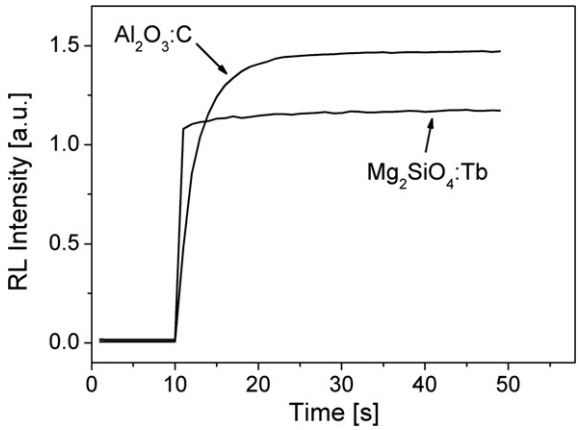

Fig. 1. Radioluminescence signal as function of time corresponding to the Al_2O_3:C- and the Mg_2SiO_4:Tb-based probes. Measurements have been made at 5 mm depth in a water phantom employing a 10×10 cm^2 irradiation field at a ^{60}Co source.

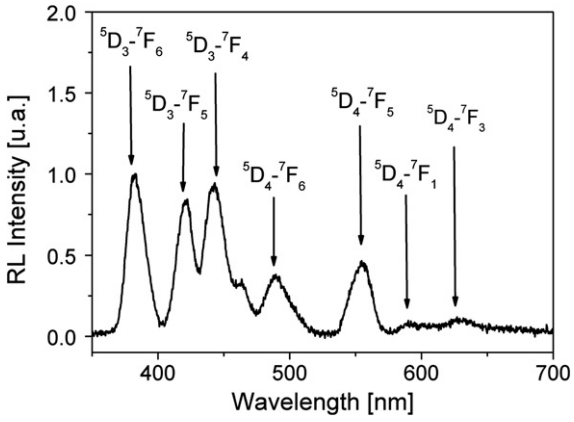

Fig. 3. RL spectrum of the Mg_2SiO_4:Tb probe. The sensitive end has been positioned at 5 mm depth in water phantom at a distance of 80 cm SSD from the ^{60}Co source. The characteristic emission lines of Tb^{3+} have been identified.

been recorded and the mean value V_f of the RL intensity over the last 10 s of the RL curve has been computed. In principle, the value of V_f can be regarded as proportional to the dose rate (Mones et al., 2006). The value of V_f as function of the cycle number is shown in Fig. 2. It is apparent from the figure that the RL response increases slightly as function of the accumulated dose. In particular, the signal increases only 0.4% after eight consecutive measurements. The abrupt fall of the RL signal observed in the second experimental point in Fig. 2 could be caused by unavoidable miss-positioning of the ^{60}Co pellet of the Theratron 80 during irradiation. The error bars in Fig. 2, which have been computed as the standard deviation of the average of the RL readings, only amount to roughly 0.1% of V_f.

The RL emission spectrum of the Mg_2SiO_4:Tb FOD probe under ^{60}Co gamma irradiation is shown in Fig. 3. As can be seen, the RL spectrum shows the characteristic lines associated with the $^5D_3 \rightarrow {}^7F_J$ ($J = 0, \ldots, 6$) transitions of the Tb^{3+} ion, indicating that Tb^{3+} sites act as luminescence centers during the RL process, as observed in other radiation-induced phenomena in this compound (Bos et al., 2006; Mittani et al., 2008). The most intense emission peaks in Mg_2SiO_4:Tb appear in the wavelength range where the stem effect emission is predominant, say, between 350 and 500 nm (De Boer et al., 1993). This situation precludes the use of the simple optical filtering technique to remove the spurious contribution of the stem effect in this case. However, the temporal separation technique proposed by Clift et al. (2002) could be a useful alternative if the Mg_2SiO_4:Tb-based FOD probe is used for dosimetry in LINACs, deserving this possibility further investigations.

The RL response of the Mg_2SiO_4:Tb-based FOD probe as function of the dose rate has been investigated. In this case the measurements have been performed in air by placing the sensitive end of the FOD probe at different distances from the ^{60}Co source and recording the RL curve at each position going from 0.14 up to 0.60 Gy min^{-1}. The absolute dose rate has been recorded at the same points by means of the ionizing chamber. In each case the FOD extreme and the ionization chamber have been placed in the center of a constant field size (10×10 cm^2). In Fig. 4 the value of V_f as function of the dose rate measured with the ionization chamber is shown. As can be seen from the figure the RL response of the Mg_2SiO_4:Tb-based FOD probe depends linearly on the dose rate within the investigated range. In particular, the maximum discrepancy is 4% at 0.2 Gy min^{-1}. The change in the response of the RL probe shown in Fig. 2 could not be responsible for this discrepancy in principle, since it is one order of magnitude less

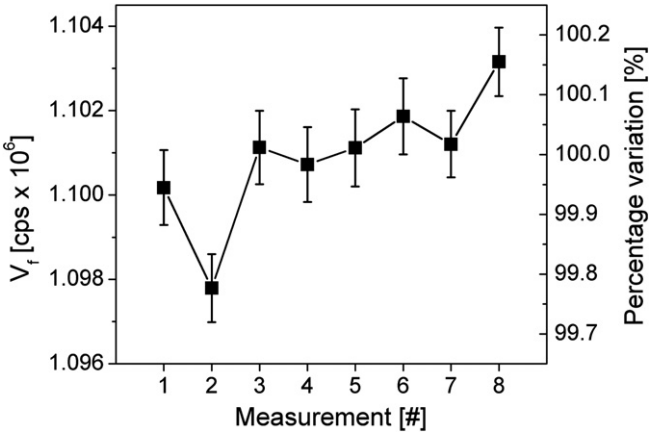

Fig. 2. Repeatability of the radioluminescence yield (V_f). The sensitive end of the optical fiber has been positioned at a distance of 80 cm from ^{60}Co source with an irradiation field of 10×10 cm^2. Sixty seconds of exposure have been used for each measurement and 120 s elapsed between consecutive measurements. Percentage variations can be appreciated on the right vertical axis, where normalization by the mean V_f value has been applied.

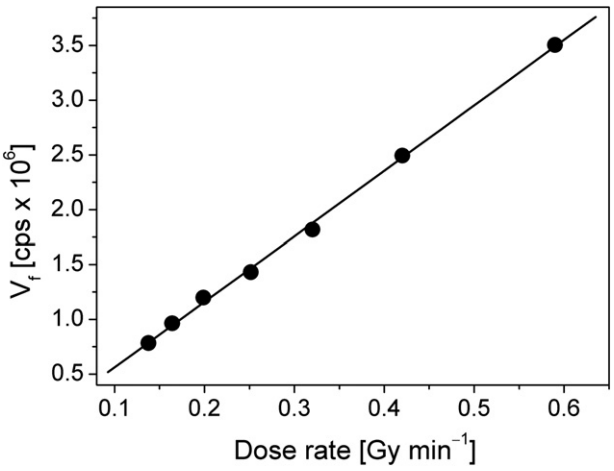

Fig. 4. Dose-rate response of the Mg_2SiO_4:Tb probe measured in air from 0.1 up to 0.6 Gy min^{-1} (circles) in a ^{60}Co radiotherapy facility. The solid line has been obtained with an ionization chamber in identical conditions. The error bars corresponding to the RL measurements are smaller than the symbol size.

important (0.4%). Although the linear response is an encouraging result, deriving the dose rate from the asymptotic value of the RL signal could preclude in principle the use of Mg_2SiO_4:Tb RL probes in cases where the dose rate is not constant. However, the dosimetry system could be employed in non-constant dose-rate conditions if an on-line correction strategy is implemented, based on the concept put forward in (Damkjær et al., 2008).

Studying the performance of the Mg_2SiO_4:Tb FOD probe when tested in protocol conditions is of interest if its application in routine radiotherapy dosimetry is envisaged. In this context, obtaining the PDD curve is probably one of the most relevant experiments to be performed, since it is useful to elucidate whether the detector shows a water-equivalent response. In order to obtain the PDD profile the RL emission of the Mg_2SiO_4:Tb FOD probe has been recorded at different depths in the water phantom and the corresponding value of V_f has been computed. In Fig. 5 the value $(100 \times V_f/V_{f,MAX})$ is plotted as function of the water depth, being $V_{f,MAX}$ the maximum V_f value. A first set of measurements have been made by going from the water surface downwards the phantom bottom (hollow circles) and a second set of measurements has been immediately performed in the upward direction (filled circles). For the sake of comparison, a second PDD curve has been recorded in identical conditions by employing the ionization chamber (solid line). As expected for ^{60}Co photons, the PDD obtained with the ion chamber reaches its maximum at 5 mm water depth and decreases monotonically at deeper depths (Johns and Cunningham, 1983). The PDD points obtained with the RL probe at higher depths match almost exactly the PDD curve corresponding to the ionization chamber. In fact, a maximum discrepancy of 1.5% is observed in the last point at 100 cm water depth. Besides, no appreciable change in the RL response of the probe as a result of accumulated dose is observed, say, points recorded downward and upward lie on the line corresponding to the ion chamber PDD. This result demonstrates that, at least for ^{60}Co photons, the Mg_2SiO_4:Tb FOD probe have a response similar to water showing no appreciable dependence on accumulated dose. Discrepancies between the response of the FOD probe and the ion chamber in the build-up region might be related to the different size and effective atomic of both kinds of detectors, as observed by other authors (Sidhu, 1999; Aznar et al., 2004; Pena et al., 2006; Song et al., 2006).

Another important characteristic of the FOD probe, which has been investigated in this work, is its performance when measuring the value of V_f for different field sizes. Fig. 6 shows the variation of

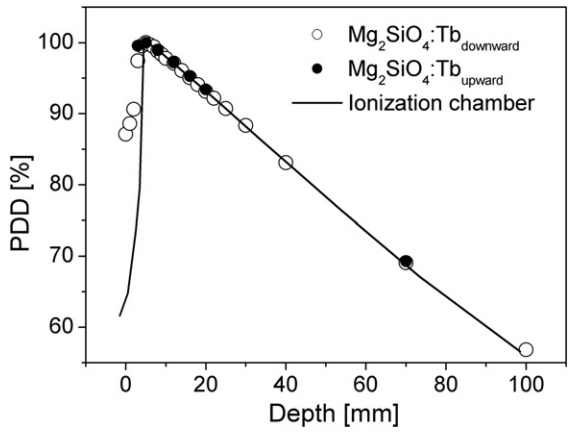

Fig. 5. Percentage depth dose obtained with the Mg_2SiO_4:Tb probe in a water phantom with an SSD equal to 80 cm and a field size of 10×10 cm^2. Downward (hollow circles) and upward (filled circles) measurements are compared with the PDD obtained with an ionization chamber (solid line). The error bars corresponding to the RL measurements are smaller than the symbol size.

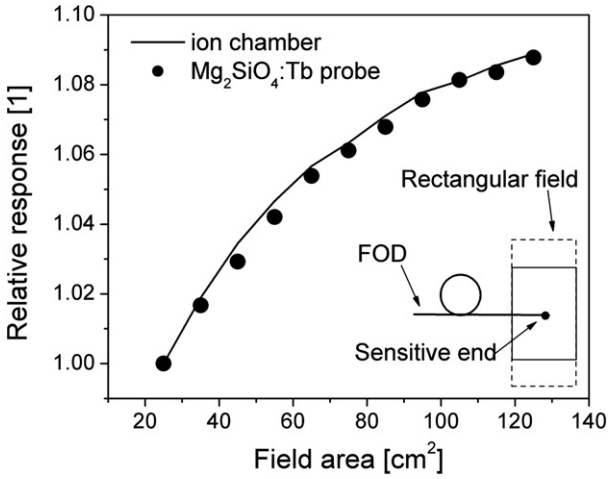

Fig. 6. Relative variation of the RL (V_f) signal (circles) as a function of the field size compared with the results obtained with an ionization chamber (solid line). The inset represents the schematic experimental setup used to carry out the measurements. The error bars corresponding to the RL measurements are smaller than the symbol size.

V_f (filled circles) with respect to the field area. The measurements have been performed in water by placing the sensitive end of the FOD probe at 5 mm depth and being the water surface at 80 cm from the ^{60}Co source. The field sizes ranged sequentially from 5×5 cm^2 up to 25×5 cm^2. The response of an ionization chamber operating in current mode has been recorded in identical conditions (solid line). In both cases, the plotted values have been normalized to the corresponding response at the smallest field size. As can be seen from the figure, a good agreement between both sets of measurements is obtained. In particular, a maximum discrepancy of 0.5% at a field size of 9×5 cm^2 is observed.

4. Conclusion

In this paper the RL characteristics of a Mg_2SiO_4:Tb-based FOD probe have been investigated for the first time. It has been shown that the FOD probe features good repeatability and linear dose-rate response under gamma irradiation at a ^{60}Co therapy source. The absolute RL yield of the Mg_2SiO_4:Tb probe is of the same order of magnitude as that of a Al_2O_3:C-based RL probe. The RL spectrum confirms that Tb^{3+} sites act as luminescence centers during the RL process.

It has been found a very good agreement between the PDD curves determined with the Mg_2SiO_4:Tb probe and a standard ionization chamber. Similar results have been obtained in varying field size experiments. Besides, the dose-rate response of the FOD probe has shown to be linear in the range of 0.1–0.6 Gy min^{-1}.

Summarizing, this work demonstrates the feasibility of employing terbium-doped sintered silicates as a FOD RL phosphor for dose assessment encouraging further research.

Acknowledgements

We would like to thank Dr. Caselli for useful discussion on the subject. This work was partially supported by grant PICT Nr. 1907 (ANPCyT, Argentina).

References

Andersen, C.E., Marckmann, C.J., Aznar, M.C., Botter-Jensen, L., 2006. An algorithm for real-time dosimetry in intensity-modulated radiation therapy using the radioluminescence signal from Al_2O_3:C. Radiat. Prot. Dosimetry 120 (1–4), 7–13.

Archambault, L., Beddar, A., Gingras, L., 2006. Measurement accuracy and Cerenkov re-moval for high performance, high spatial resolution scintillation dosimetry. Med. Phys. 33, 128.

Aznar, M.C., Andersen, C.E., Bøtter-Jensen, L., Bäck, S.Å.J., Mattsson, S., Kjær-Kristoffersen, F., Medin, J., 2004. Real-time optical-fibre luminescence dosimetry for radiotherapy: physical characteristics and applications in photon beams. Phys. Med. Biol. 49, 1655–1669.

Aznar, M., Hemdal, B., Medin, J., 2005. In vivo absorbed dose measurements in mammography using a new real-time luminescence technique. Br. J. Radiol. 78, 328–334.

Bhasin, B.D., Sasidharan, R., Sunta, C.M., 1976. Preparation and thermoluminescent characteristics of terbium doped magnesium orthosilicate phosphor. Health Phys. 30, 139–142.

Beddar, A.S., 2007. Plastic scintallation dosimetry and its application to radiotherapy. Radiat. Meas. 41, S124–S133.

Bos, A.J.J., Prokic, M., Brouwer, J.C., 2006. Optically and thermally stimulated luminescence characteristics of MgO:Tb^{3+}. Radiat. Prot. Dosimetry 119 (1–4), 130–133.

Clift, M.A., Johnsoton, P.N., Webb, D.V., 2002. A temporal method of avoiding the Cherenkov radiation generated in organic scintillator dosimeters by pulsed mega-voltage electron and photon beams. Phys. Med. Biol. 47, 1421–1433.

Damkjær, S., Andersen, C., Aznar, M., 2008. Improved real-time dosimetry using the radioluminescence signal from Al_2O_3:C. Radiat. Meas. 43, 893–897.

De Boer, S.F., Beddar, A.S., Rawlinson, J.A., 1993. Optical filtering and spectral measurements of radiation-induced light in plastic scintillating dosimetry. Phys. Med. Biol. 38, 945–958.

Erfurt, G., Krbetschek, M.R., 2002. A radioluminescence study of spectral and dose characteristics of common luminophors. Radiat. Prot. Dosimetry 100, 403–406.

Frelin, A., Fontbonne, J., Ban, G., 2006. A new scintillating fiber dosimeter using a single optical fiber and a CCD camera. IEEE. Trans. Nucl. Sci. 53, 1113.

Johns, H.E., Cunningham, J.R., 1983. The Physics of Radiology, Fourth ed. Charles C Thomas Publisher, New York.

Justus, B., Falkenstein, P., Huston, A., 2004. Gated fiber-optic-coupled detector for in vivo real-time radiation dosimetry. Appl. Opt. 43, 1663.

Marcazzó, J., Henniger, J., Khaidukov, N.M., Makhov, V.N., Caselli, E., Santiago, M., 2007. Efficient crystal radiation detectors based on Tb^{3+}-doped fluorides for radioluminescence dosimetry. J. Phys. D: Appl. Phys. 40, 5055–5060.

Marckmann, C., Aznar, M., Andersen, C., 2006. Influence of the stem effect on radioluminescence signals from optical fibre Al_2O_3:C dosemeters. Radiat. Prot. Dosimetry 119, 363–367.

Mittani, J.C., Prokic, M., Yukihara, E.G., 2008. Optically stimulated luminescence and thermoluminescence of terbium-activated silicates and aluminates. Radiat. Meas. 43, 323–326.

Mones, E., Veronese, I., Moretti, F., 2006. Feasibility study for the use of Ce^{3+}-doped optical fibres in radiotherapy. Nucl. Instrum. Methods Phys. Res. A 562, 449–455.

Pena, J., Sánchez-Doblado, F., Capote, R., Terrón, J.A., Gómez, F., 2006. Monte Carlo correction factors for a Farmer 0.6 cm^3 ion chamber dose measurement in the build-up region of the 6 MV clinical beam. Phys. Med. Biol. 51, 1523–1532.

Prokic, M., Yukihara, E.G., 2008. Dosimetric characteristics of high sensitive Mg_2SiO_4:Tb solid TL detector. Radiat. Meas. 43, 463–466.

Sidhu, N.P.S., 1999. Interfacing a linear diode array to a conventional water scanner for the measurement of dynamic dose distributions and comparison with a linear ion chamber array. Med. Dosim. 24, 57–60.

Song, H., Ahmad, M., Deng, J., Chen, Z., Yue, N.J., Nath, R., 2006. Limitations of silicon diodes for clinical electron dosimetry. Radiat. Prot. Dosimetry 120, 56–59.

Yukihara, E.G., Whitley, V.H., Polf, J.C., Klein, D.M., McKeever, S.W.S., Akselrod, A.E., Akselrod, M.S., 2003. The effects of deep trap population on the thermoluminescence of Al_2O_3:C. Radiat. Meas. 37, 627–638.